General Disclaimer

One or more of the Following Statements may affect this Document

- This document has been reproduced from the best copy furnished by the organizational source. It is being released in the interest of making available as much information as possible.

- This document may contain data, which exceeds the sheet parameters. It was furnished in this condition by the organizational source and is the best copy available.

- This document may contain tone-on-tone or color graphs, charts and/or pictures, which have been reproduced in black and white.

- This document is paginated as submitted by the original source.

- Portions of this document are not fully legible due to the historical nature of some of the material. However, it is the best reproduction available from the original submission.

OLD DOMINION UNIVERSITY RESEARCH FOUNDATION

DEPARTMENT OF PHYSICS AND GEOPHYSICAL SCIENCES
SCHOOL OF SCIENCES
OLD DOMINION UNIVERSITY
NORFOLK, VIRGINIA

X-RAY EMISSION FROM HIGH TEMPERATURE PLASMAS

By

Wynford L. Harries

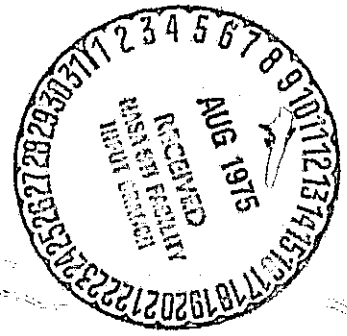

Annual Report

Prepared for the
National Aeronautics and Space Administration
Langley Research Center
Hampton, Virginia

Under
NASA Research Grant NSG 1022

July 1975

CONTENTS

Annual Report

NASA Grant NSG-1022

X-ray Emission from High Temperature Plasmas

by

W. L. Harries[1]

The investigation is a continuation of contract NAS1-11707-23 and covers the period 1 July 1974 to 30 June 1975. It was carried out using the experimental facilities at NASA Langley Research Center.

The purpose of the work was to investigate the physical processes occurring in Plasma Focus Devices. These devices produce dense, high temperature plasmas and emit x rays of hundreds of KeV energy and 10^9-10^{10} neutrons per pulse. An understanding of the mechanisms involved would be helpful in explaining solar flare phenomena, and would be of interest for controlled thermonuclear fusion applications. The high intensity, short duration bursts of x rays and neutrons could also possibly be used for pumping x-ray or neutron lasers, respectively.

Two plasma focus devices exist at Langley--Focus I, on which all the measurements were made, and Focus II. Considerable difficulty has been experienced on Focus II, essentially in synchronizing the spark gaps, and the period September through December 1974 was spent entirely carrying out engineering tests on it, the details of which are not included here. Focus II should be operational shortly.

The specific objective of the work on Focus I was to investigate the x-ray emission. In brief, a model which is not complete is proposed to explain the x-ray behavior. The model assumes that the plasma is compressed

---

[1] Professor of Physics, Old Dominion University, Norfolk, VA 23508.

by the magnetic field, which then pinches off the current. The magnetic energy is then converted to electric energy and a region of high electric field is created between the dense plasma and the anode. Electrons are accelerated in this field to energies of up to order 100 KeV, and Bremsstrahlung x rays are emitted both from the plasma, and from the anode surface. Estimates of the plasma "temperature" are about 3 KeV, so low energy x rays emerge from the plasma blob while the high energy component is emitted from the anode. The concept of a dense plasma blob and a sheath with high electric fields seems consistent with a model of neutron production, proposed previously by J. H. Lee, et al.[1] -- the converging beam model. The results of the work have been written up as a paper to be submitted to Physics of Fluids (Appendix A).

Evidently the x-ray production and neutron production should be interrelated and further experiments were made to test the above conclusions, based both on x-ray and neutron measurements.

To test whether the electron trajectories were correct, a method was devised to show the direction and possibly angular spread of the electron velocity vectors (Appendix B). The experiment seems to confirm the above model.

Measurements were also carried out to determine where in the focus the neutrons originate, to check whether they could be produced by ions accelerated by the same electric field as accelerated the electrons. Details of the method are given in Appendix C.

The grant has been refunded for the period 1 July 1975 to 30 June 1976, and a number of further experiments are planned and details are given in

---

[1] Lee, J. H., L. P. Shomo, M. D. Williams, and H. Hermansdorfer, Phys. Fluids 14, 2217 (1971).

Appendix D. These include a measurement of x-ray emission vs. space and time, measurement of neutrons vs. space and time using time-of-flight separation, a recheck of neutron emission vs. angle from the axis using thermoluminescent detectors, and possible time-of-flight ion velocity analyzer.

The work was carried out in collaboration with Dr. J. H. Lee of Vanderbilt University, who is working under NASA Grant NGR 43-002-031, and D. R. McFarland of NASA, and their help is gratefully acknowledged.

BIBLIOGRAPHY

1. "Fine Structure of hard X-ray Emission from a Plasma Focus Apparatus" W. L. Harries, J. H. Lee, and D. R. McFarland, Bull. Am. Phys. Soc. 19, 511, (1974).

2. "Space and Time Resolved Observations of X-ray Production in a Plasma Focus Apparatus," J. H. Lee, W. L. Harries and D. R. McFarland, First IEEE International Conference on Plasma Science, Knoxville, Tennessee, 15-17 May 1974, Paper 2C11.

3. "Electron Dynamics in a Plasma Focus Based on X-ray Measurements," W. L. Harries, J. H. Lee, and D. R. McFarland, Bull. Am. Phys. Soc. 19, 945 (1974).

4. "Electron Dynamics in a Plasma Focus," W. L. Harries, J. H. Lee, and D. R. McFarland, submitted to Physics of Fluids.

APPENDIX A

ELECTRON DYNAMICS IN A PLASMA FOCUS

Wynford L. Harries
Department of Physics,
Old Dominion University, Norfolk, Virginia 23508

J. H. Lee
Department of Physics and Astronomy,
Vanderbilt University, Nashville, Tennessee 37235

and

Donald R. McFarland
NASA Langley Research Center, Hampton, Virginia 23665

ABSTRACT

The intensity of x rays from a plasma focus was measured as a function of position of emission, time, energy and angle, with resolution in several of these variables simultaneously. The low energy x rays emanated from the dense focus region, but the high-energy components were mostly from the anode. Emission from the focus occurred some 20 ns prior to that from the anode, but the latter continued for 500 ns. Spatial estimates of electron energy were made; the electrons appeared to gain energy as they traveled from the plasma focus toward the anode, and possessed an "average" energy of about 10 keV near the anode surface. The time integrated intensity was also measured versus the angle θ from the axis of symmetry for $0 < \theta < \pi/2$ and for $\theta = \pi$, or behind the anode, in three energy ranges. Considerable anisotropy was revealed; the polar diagram of medium energy ($\simeq$ 20 keV) x rays resembled a cardioid, but that for higher energy ($\simeq$ 100 keV) showed a lobe into the anode, with a forward-to-back ratio of about 50, indicating the plasma was near collisionless with run-away relativistic electrons in severely anisotropic velocity distributions. By considering Bremsstrahlung emission from relativistic electrons, an explanation is suggested for the radiation patterns, and conversely the patterns are used to invoke the electron trajectories. The electron trajectories are consistent with the results of the spatial energy analysis. The electric fields required to produce such electron trajectories are also consistent with the converging beam model of neutron production, proposed previously.

I. INTRODUCTION

The investigation of dense, high-temperature plasmas is of interest both in astrophysics and in the controlled thermonuclear fusion program. Such plasmas, sufficiently dense and energetic to emit neutrons and x rays, can be obtained from plasma-focus devices.[1-9]

Measurements of the soft x radiation from a focus had previously been reported by Peacock et al. in the range below 10 keV.[10] They were able to record the spectra from seventeen-times ionized argon introduced into the deuterium, and from an estimate of the stripping time required inferred that the density of the plasma was about 10^{19} cm^{-3}. Also, by measuring the transmission of x rays through foils of various thicknesses, they estimated an electron temperature of about 2.5 keV in pure deuterium. Bernstein et al.[11] have reported measurements in space, time, and energy of x-ray emission in the 7 to 29 keV range. They found the photon energy distribution function obeyed a power law dependence, proportional to E_p^{-2}, where E_p is the photon energy and suggested that the high-energy x rays arose from accelerated electrons. The hard x-ray spectrum ($>$ 100 keV) from a plasma focus has been studied by Lee et al. who measured the spectral distribution with nuclear emulsions.[12] In this range, the best fit for the electron energy distribution function was a power law, $f(E) \propto E^{-\gamma}$ with γ about 4, again suggesting that there was a nonthermal component of electrons in the plasma. Studies of the angular dependence of the intensity of x rays had revealed anisotropy, with a reduced signal on axis,[9] which has not been explained.

The purpose of this investigation was to make an extended study of the Bremsstrahlung x rays from a plasma focus, and in particular to analyze the emission versus position, time, energy, and angle of emission. The previous results on angular dependence[9] are confirmed here, and considerably extended by a different technique. In addition, we find a different behavior for low energy ($\simeq$ 20 keV) and high energy ($\simeq$ 100 keV) emission.

Section II describes the experimental method, and Section III the results. In Section IV, an explanation is offered for the experimental behavior, and conversely the results are invoked to yield information on the particle dynamics in the plasma, and mechanism of x-ray emission. The picture that emerges seems consistent with a previously proposed mechanism of neutron production.

II. EXPERIMENTAL METHOD

A. Plasma-Focus Device

The plasma-focus device, reported elsewhere,[8,9] consists of coaxial cylindrical electrodes, 23 cm long, with a cathode of 10 cm diameter, and an internal anode of 5 cm diameter, both of copper (Fig. 1). They are enclosed in an aluminum sphere of 2 mm wall thickness and 30 cm diameter. The filling gas was deuterium at about 7 Torr. A 125 μF capacitor bank, charged to 20 kV, provides 25 kJ energy. During the "focus" stage, the plasma is compressed into a volume $\simeq 10^{-2}$ cm^3, with densities $\simeq 10^{19}$ cm^{-3}, and electron temperatures of several kilovolts. Copious neutrons, $\simeq 10^{10}$ per focus are produced as well as x rays of over 100 keV.[8,9]

B. Methods of Measurement

The main results here are based on measurements of x-ray intensity. In addition, numerous diagnostics, such as image converter cameras in both streak and framing modes observing the visible radiation were used.[6] For the x-ray measurements spatial resolution was obtained using pin-hole techniques, time resolution using scintillators-photomultipliers, and energy resolution using filters; combinations of these techniques were used to solve for more than one variable simultaneously. Measurements were also made versus angle from the axis, and for different energy ranges.

The pinhole cameras were designed with three pinholes to provide both spatial information and energy resolution versus position by using filters. Each pinhole was 0.4 mm diameter (minimum) in a 2 cm thick lead housing. The pinholes were placed adjacent to the outside surface of the vacuum vessel, about 15 cm from the focus, with the image sensor 15 cm behind them (Fig. 1). The filters enabled both qualitative and quantitative estimates of the x-ray energy and the energy (or temperature T_e, if a Maxwellian distribution existed) of the electrons in the plasma. The filter material chosen was lead, which has a high absorption coefficient, so the filters could be thin. Hence, the volume in which an x ray could be scattered by the absorber was small, and multiple scattering reduced, a factor that would improve the imaging of the x-ray patterns. There was sufficient x-ray intensity so that measurements could be made through the aluminum vacuum vessel 2 mm thick, as well as the lead filters.

It is convenient to describe the filter characteristics. The linear absorption coefficient μ for x rays depends strongly on E, the x-ray

energy, and for most materials except at the K, L . . . absorption edges

$$\mu(E) = A_n E^{-3} \qquad (1)$$

where A_n is a constant for the material A, and the subscript depends on whether E lies above or below the K, L . . . edges. For example, for lead, above the K edge at 89 keV, $A_1 = 6.35 \times 10^7$ ($cm^{-1}keV^3$) (E in keV, μ in cm^{-1}); from 89 down to 15 keV, $A_2 = 9.5 \times 10^6$; from 15 to 13.1 keV, $A_3 = 3.94 \times 10^6$, etc. As the contribution transmitted below 15 keV is small, only A_1 and A_2 will be used. For aluminum, the constant 7.3×10^4 was used over the above range. The transmission function T(E) for several filters of materials, A, B ... in series, is then $\exp -(A_n x_A + B_n x_B + \ldots)/E^3$ where A_n, B_n . . . are the appropriate constants denoting materials, A, B . . . of thickness x_A, x_B . . . .

If we assume the plasma has a Maxwellian distribution of electron velocities, and that the free-free electron emission coefficient is of the form given by Kramers,[13] then the intensity of x-ray emission from unit volume of plasma per sec in the energy range E to E + dE is given by

$$I(E)dE = \text{const. } n_e n_i Z^2 T_e^{-1/2} \exp(-E/KT_e)dE \qquad (2)$$

Here n_e and n_i are the electron and ion densities, Z is the atomic number of the ions, E the x-ray energy, K Boltzmann's constant and T_e the electron temperature of the plasma. The function I(E)T(E), the transmitted intensity per unit energy, is shown in Fig. 2(a) for electron temperatures of 5 and10 keV, with filters of 2 mm of aluminum

plus 102, 229, 508, and 762 μm of lead, respectively. The results are equivalent to a band-pass filter in energy, with the lower energy edge dependent mostly on the thickness of the filtering materials, while the high-energy edge depends on the energy distribution function of the electrons. The peak value occurs at an energy $E_{max,\,n}(\text{keV}) = \{3\ KT_e(A_n\ x_A + B_n\ x_B + \ldots)\}^{1/4}$, with KT_e in keV. The subscript n shows that there can be several maxima, one for each different A_n; however, the maxima may not exist if the calculated value of $E_{max,\,n}$ lies outside the energy range in question.

The total intensity I_T transmitted in the energy range E_p to E_q for several filters in series is then

$$I_T = \int_{E_p}^{E_q} I(E)\ T(E)\ dE \qquad (3)$$

and is the sum of such integrals over several energy ranges involving different constants. Equation (3) was integrated by computer using Simpson's rule, for six values of T_e, namely, 3, 5, 10, 15, 20, and 25 keV, (values encompassing the probable plasma temperature), and for the above filter combinations. The integrand approaches zero at low and high energies so that the range of integration was from nine to several hundred keV in steps of 1 keV. The resultant curves of I_T versus lead thickness depended strongly on T_e, and for T_e = 10 keV qualitatively agreed with the measured dependence on filter thickness.

If the ratio R of the signal through one filter thickness to that of the signal through a different thickness is taken, R depends strongly on T_e. Therefore, an estimate of T_e can be made by measuring

R. In Fig. 2(b), the inverse function T_e versus R is plotted for two different filter combinations, and it can be seen that a fairly accurate value of T_e can be obtained even if R is only roughly known. Similar calculations have been made by Elton et al.[14]

The use of ratios is advantageous in four respects: (a) If the readings are measured from the same point in the plasma, R is independent of the plasma density (see Eq. (2) and (3)) as $n_e n_i Z^2$ cancels; (b) It is independent of impurities in the plasma, important for a plasma focus, because with impurities we would replace $n_e n_i Z^2$ with $n_e(n_1 Z^2_1 + n_2 Z^2_2 + \ldots)$ where n_1, n_2 . . . are the densities of the various ions of charges Z_1, Z_2 . . . and the expression cancels; (c) Taking a ratio precludes an absolute calibration of the sensor recording the x rays; (d) It would give some measure of T_e even if the x-ray emission came from the anode, as we would then write $n_e n_A Z^2_A$ where n_A and Z_A are the density and atomic number of the anode ($N_A \approx 10^{22}$, $Z_A = 29$) and the expression cancels. Thus, R would yield an estimate of T_e, or if a maxwellian distribution of electron energies did not occur, would indicate qualitatively a higher or lower average energy. In addition, it is assumed that the response of the sensor is independent of photon energy and is linear with x-ray intensity.

The sensors for (time integrated) spatial resolution of x rays were (1) x-ray intensifying screens with Polaroid film, (2) x-ray film, and (3) thermoluminescent detectors.

The x-ray intensifying screens were DuPont Chronex, Lightning type, and Polaroid 3000 ASA film was placed behind them to make a contact print. The combination could record the x rays from a single

discharge through the vacuum vessel and lead filters, or a series of discharges could be superimposed. However, only qualitative estimates of x-ray intensity could be made because the response of the screen-film combination was not absolutely calibrated.

Quantitative estimates of intensity could be made using Kodak x-ray film and a densitometer, but here, thermoluminescent detectors (TLD) were used mainly.[15] These are crystals of 1/8 in. x 1/8 in. x 1/32 inch which, when irradiated with x rays, can store some of the energy in metastable states. Some of this energy can be recovered later as visible photons when the material is heated and measured in a commercially available analyzer.[16] Its large dynamic range, (10^7), enabled the detectors to be used for a single pulse or to integrate the effects of many pulses. Several types of detectors were investigated: Harshaw type 700, more sensitive to x rays than neutrons, but too insensitive here; type 600, which measured mainly neutrons; and type 400, which measured both. A comparison of the contribution from x rays versus neutrons to the readings was made by using filters of lead with and without boron-filled polyethylene, which strongly absorbs neutrons. The results indicate that the TLD 400 output signal is approximately proportional to the x-ray irradiation, and this type was used for the results that follow. Also, 18 such detectors exposed simultaneously gave outputs within ±5 percent.

The response of the TLD type 400 detectors in different energy ranges was measured by placing two of them in series so that the second TLD could sense only the x-ray flux transmitted through the first. If the doses on the first and second TLD were S_1 and S_2, then the fraction of the x-ray energy retained and measured in each TLD is given by $\eta = 1 - S_2/S_1$.

Values of η were found to be 0.49 ± 0.05 for 2 mm aluminum alone, decreasing to 0.15 ± 0.06 for 2 mm aluminum plus lead filters thicker than 200 μm. Assuming $T_e = 5$ keV, the absorbers could be regarded as band-pass filters, ranging from 15-25 keV halfwidth for the aluminum to 50-75 keV for aluminum plus 762 μm of lead (Fig. 2); hence, η was constant for energies above about 30 keV, and possibly higher at lower energies. To see if backscattering of lower energy x rays into the rear TLD affected the values of η, the results were checked both with a lead surface behind and adjacent to the rear TLD, and also with the lead surface removed about 2 cm away and shielded with aluminum, a good absorber. The readings were approximately equal, indicating backscatter was unimportant.

III. EXPERIMENTAL RESULTS

Triple-pinhole camera pictures of a typical discharge observed through the vacuum vessel at $\theta = 80°$ (Fig. 1) are shown in Fig. 3(a) with the middle and upper pictures taken through filters of 102 and 254 μm of lead. The spatial resolution is adequate, and x-ray emission is visible from the plasma about 2 cm above the anode, from a region about 1 mm wide at the top extending downward in a cone with the intensity greater near the anode surface, and concentrated at the center. The aluminum vessel alone transmitted x rays >15 keV, while the 102 and 254 μm filters transmitted x rays >20 and 30 keV, respectively. By comparing the ratio of the intensities point by point, we found that the filters reduced the emission from the plasma focus to a greater extent than that from the anode surface, suggesting that the electron energy was greater at the anode surface than in the dense focus region. Furthermore, we note that the emission from

the plasma is increasing between the focus and the anode surface, where the density may be decreasing. This suggests that the electrons increase their energy as they approach the anode.

First, an estimate of a space-averaged electron temperature was made by recording the x rays on TLD's, to obtain the intensity ratio R for the filter combinations A and B of Fig. 2(b). The measured curves of x-ray intensity from the whole plasma versus lead thickness are in good agreement with Eq. (3) for KT_e = 10 keV. However, for such high electron energies, electron velocity distributions other than Maxwellian may give a similar curve. For example, a power-law distribution $I(E) = \text{const } E^{-4}$ also shows similar behavior. Therefore, it cannot be determined whether or not the signals were due to a "nonthermal" component of electrons.[12] The x rays from 65 focuses were superimposed on TLD's at $\theta = 80°$ and values of R were 37 and 8 for filter combinations A and B, indicating values of T_e of 9 and 11 keV, respectively, assuming η is independent of E. If a correction for η is made, T_e becomes 16 keV from curve A and 8 keV from curve B.

As the plasma may have regions of different "temperatures," two 9 x 9 rasters of TLD's were placed behind pinholes to obtain spatial resolution. The rasters were placed at $\theta = 80°$ and exposed to 25 focuses, one observing through the vacuum vessel wall and the other through a filter of 254 μm of lead in addition. Simultaneously, the plasma x rays were photographed on Polaroid film through similar filters. The results are compared in Fig. 3(c) and (d) where the rasters

have been slightly enlarged with respect to the film image, and good correspondence is observed. Where a blank is shown, the TLD reads zero. The highest reading in the lower raster corresponds to the same point as the highest reading in the upper. Numerical estimates of local T_e can be made from point-by-point ratios of the TLD readings. These reveal the variations of T_e in two dimensions. The values of T_e near the anode were about 9 keV, dropping off to about half this value 0.5 cm horizontally away from the axis. The vertical dependence of T_e was not clear; one run of about 25 focuses indicated that T_e dropped to about 5 keV at a distance of about 3 mm above the anode, but the run in Fig. 3, for a similar number of focuses, suggests T_e was still about 10 keV for a distance of 6 mm above the anode. It was not possible to determine T_e at the focus region about 2 cm above the anode, as the readings of the upper raster in Fig. 3(c) were too small. Results from rasters at $\theta = 15°$ also indicated that the horizontal spread of highest temperature region was within about 0.5 cm of the vertical axis.

The values of about 10 keV from the anode region are higher than the values of 3 to 5 keV generally quoted for a plasma focus. The estimate from the anode surface may be too high due to penetration of the electrons deep into the cavity of the copper cap before releasing x rays, which would have to traverse some thickness of copper before striking the TLD's at $\theta = 80°$. To account for this effect, T_e versus R curves have been recalculated with an extra 100 μm of copper placed in front of both sets of filter combinations A and B, as shown by the curves A' and B' (Fig. 2(b)). Readings of T_e measured with the extra copper

are lower for the same R. The error is negligible if combination B is used and $R < 10$. Also, the value of η was the same for both filters in combination B, and, hence, the values of around 9 keV near the anode surface seem reasonable. Examination of Fig. 3 suggests most x rays originate on or near the anode, and would give the main contribution to "space-averages" values of T_e.

Since pinhole camera pictures only provided time-integrated information, a method was devised which combined the space resolution of a pinhole camera with the time resolution of a photomultiplier-oscilloscope system. To monitor intensity variations versus time at different positions on the x-ray image, two light guides made of polished aluminum tubes were placed behind the intensifying screen (Fig. 1, camera L) and aligned on the middle of the three images. Commercially available fiberglass light pipes were not suitable because they become fluorescent from the x rays and neutrons unless adequately shielded. In Fig. 4, P and e denote image points corresponding to the plasma focus and the electrode, respectively, and the light signals were directed to two photomultipliers, whose outputs were displayed on an oscilloscope in Fig. 4(c). It can be seen that x-ray emission from the plasma focus occurs about 20 ns ahead of emission from the electrode. Emission from the electrode continues for more than 500 ns, and well into and during vaporization of the copper electrode material. For a 50 keV electron, the time needed to reach the electrode surface from the focus position 1.5 cm above, is only a fraction of a nanosecond. This discrepancy may be important for understanding the mechanism for plasma-focus formation, and will be discussed later.

Most of the measurements above were made approximately on or off axis, but as anisotropy had been reported previously,[9] measurements were made versus angle θ from the axis. The TLD's, with an area of about 9 mm^2 and placed 15 cm from the focus, could define an angular position within about 1°. Measurements for $0 < \theta < \pi/2$ were made with the detectors placed roughly every 15° outside the aluminum sphere, such as D in Fig. 1. (The anode surface was 2.5 cm below the center of the sphere.) For $\pi/2 < \theta < \pi$ the anode and cathode shielded the detectors from radiation emanating from near the anode surface. Readings for intermediate angles between $\pi/2$ and π were not attempted, but readings for $\theta = \pi$ were obtained by placing detectors inside a hole in the anode at B.

To normalize the readings inside the anode at B with those outside the vessel at D, it was necessary to interpose the same material. First a copper cap was placed to act as the upper surface of the anode at H and detectors placed inside the vessel at A, behind a similar copper shield. Simultaneously, the readings at 0° were taken with plate C of copper, and also through the aluminum vessel at $\theta = 75°$. In a further experiment, the plates at H and C were made of aluminum, and readings taken simultaneously at B, C, and D. The plates were all 2 mm thick, similar to the vacuum wall, and the distances of the detectors from the focus were approximately 15 cm. There were no great differences in plasma-focus formation, whether copper or aluminum were used as the cap of the electrode.

The detectors were thermally insulated inside lead holders and shielded from the plasma and any vaporized metals. Comparison of measurements made inside the vessel, and outside where there was adequate cooling, indicated that the detectors lost very little of their response due to heating.

In addition to measuring x-ray emission versus θ, energy resolution was obtained using filters. The filters were the shield or vacuum vessel and, in addition, lead sheets of thickness 102, 203, 204, 508, and 762 μm, respectively. Each measurement was recorded on three TLDs except at B, where there was only one detector per filter due to lack of space.

The x-ray emissions from about 65 focuses were superimposed on the detectors and the readings recorded as intensity versus filter thickness for different θ. After normalizing the values, polar diagrams of x-ray intensity were drawn (Fig. 5(a) and (b)). All three readings for each θ are shown and the circles are for aluminum at A, B and C in Fig. 1. The pattern in Fig. 5(a) taken through 2 mm of aluminum confirms previous results[9] for $0 < \theta < \pi/2$ showing reduced intensity for $\theta = 0$, and assuming the curve is drawn correctly to the extra point at $\theta = \pi$ resembles a cardioid. The pattern in Fig. 5(b) taken through 2 mm of aluminum plus 762 μm of lead, is greatly different--a forward ($\theta = 180°$, the direction of electron-velocity vector) lobe about 50 times greater than the backward or sideways signal is evident. The polar diagrams for intermediate filters were intermediate between a cardioid and a narrow lobe.

Similar polar diagrams were obtained with copper at A, B, and C in Fig. 1. However, with no lead filter, the diagram shows a slightly forward oriented lobe as indicated with the two triangles in Fig. 5(a) which are normalized to the signal at $\theta = 45°$. With the 762 μm filter, a pronounced lobe was observed with a forward-back ratio of from 20 to 40, similar to Fig. 5(b).

For the emission measured through 2 mm of aluminum alone, x rays of as low as 15 keV are transmitted while only those over 50 keV should be observed through an additional lead filter of 762 μm. With copper, which has a higher absorption coefficient, x rays of >30 keV would be detectable with no lead filter and >60 keV with a 762 μm lead filter. Therefore, Fig. 5(a) corresponds to "medium" energies, >15 keV for aluminum, and >30 keV for copper, while Fig. 5(b) corresponds to energies over 50 keV and of order 100 keV, indicating electrons of this energy existed in the plasma.

IV. DISCUSSION

Some numerical estimates of the magneto-plasma parameters are considered next. In the dense focus, values of plasma density n_e of order 10^{19} cm^{-3} and temperatures T_e and T_i of several keV are generally accepted. The magnetic compression should make T_i greater than T_e and the ions should heat the electrons. However, an estimate of the ion-electron equipartition time yields a value larger than, but not greatly different from, the containment time of about 50 ns, and hence T_i should not be greatly different from T_e. Assuming $T_i \approx T_e = 3$ keV, then the electron self-collision time should be of order 1 ns and the ion self-collision time about 60 ns, so both electrons and ions should approach Maxwellian distributions. For these values of temperature, the plasma pressure P_{max} at the instant of greatest compression should be of order 5×10^{10} dynes/cm^2.

Both outside and inside the plasma, strong magnetic fields exist just prior to the focus, as the current is of order 10^6 A. The azimuthal magnetic field $B(r)$ surrounding the current sheet compresses

the plasma to a radius $r_o \approx 0.2$ cm, and just prior to the focus $B(r_o) \approx 10^6$ gauss corresponding to a magnetic pressure $P_B \approx 5 \times 10^{10}$ dynes $cm^{-2} \approx P_{max}$. There was an appreciable toroidal magnetic field within the plasma, and, for example, assuming constant current density, (which may not be true), $B(r) \propto r$ for $r < r_o$, and zero on axis. The magnetic field inside the plasma would be compressed with the plasma, as the resistance of the plasma at maximum compression was of order 3×10^{-7} Ωcm (about 1/5 that of copper), so the magnetic field and plasma were frozen together. Again, the diffusion time τ_o of the magnetic field over a distance r_o at $T_e = 3$ keV was 4×10^{-4} sec, much greater than the plasma containment time $\tau \approx 10^{-7}$ sec, also suggesting the plasma and magnetic field moved together.

However, even before or after the focus formation, particles should be able to escape along axis as $B(0) \to 0$. There would be few particle collisions as the coulomb cross sections of deuterium ions at $T_e = 3$ keV are of order 10^{-19} cm^2 and the electron-ion mean-free paths would be of order 1 cm, comparable or larger than the plasma dimensions. The loss of particles along axis will be of importance later in explaining the duration of x-ray emission from the anode.

The following picture is suggested for the x-ray emission. In the focus the Debye length was of order 10^{-5} cm (number of particles in a Debye sphere of order 10^4), and along axis it would not be expected that strong electric fields could exist that would accelerate the electrons. Thus, low-energy x rays would be emitted from the focus corresponding to an electron temperature of a few keV as shown in Fig. 3.

It would seem unlikely that the hard x-rays would be due to electrons in the high energy tail of a thermal distribution of a few keV. Measurements showed the hard x rays emanated from the region between the focus and the anode, and the observation of x rays of over 50 keV suggests voltage differences of this amount occur, which if applied over distances of order 1 cm, imply fields of order 5×10^4 V/cm. Then applying the criterion of Dreicer,[17] even with $n_e = 10^{19} cm^{-3}$, all electrons over 200 eV should run away. But assuming the electrons are spread out from a column of about 1 mm diameter to one of several cm diameter and, in addition, are swept into the anode by strong fields, the reduction in density from that at the focus should be several orders of magnitude, and there is even less likelihood of collision. Further, such electric fields would make the electron velocity distribution in the region between the dense focus and the anode severely anisotropic, and the electrons relativistic.

In summary, we would expect a dense plasma in the focus, as well as a less dense sheath which had an appreciable fraction of its electrons relativistic and near-collisionless with a severely anisotropic velocity distribution. The dense plasma could feed electrons near the axis into the sheath.

The anisotropy of the Bremsstrahlung intensity indicates ordered motion of the electrons, and it is assumed that they travel from the high density region in approximately straight lines, consistent with a "collisionless" plasma, and gain energy in proceeding to the anode. The pinhole pictures (Fig. 3(a) and (c)) show that the region of emission, which indicates the trajectories of the high-energy electrons, is a cone. Figure 3(b) taken from $\theta = 0°$ suggests that the highest energy electrons are on axis.

The emission of Bremsstrahlung from a directed beam of electrons is well known, and the intensity $I(\phi)$ from one electron per unit solid angle per unit time is given by

$$I(\phi) = \frac{q^2 a^2 \sin^2\phi}{16\pi^2 \epsilon_0 c^3 (1 - \beta\cos\phi)^5} \qquad (4)$$

Here q is the charge of the electron, a the value of the vector acceleration, ϵ_0 the dielectric constant of free space, c the velocity of light, and ϕ the angle of emission relative to the forward direction of the electron. Relativistic effects are included and β is the usual v/c. The radiation patterns are shown in Fig. 6(a) for different electron energies, and as $\beta \to 0$ there is no radiation forward or backward; but as β increases, the radiated power is directed predominantly in the forward direction.

Then the measured intensity at any given $\theta = \pi - \phi$ would be the sum of patterns similar to Fig. 6 from electrons in a cone whose velocity vectors were at any angle up to α relative to the axis of symmetry of the apparatus (Fig. 6). The intensity pattern vs θ at energies $\approx$20 keV would then resemble a cardioid as in Fig. 5(a), and at energies $\approx$100 keV would resemble a forward lobe as in Fig. 5(b). The pattern for copper ($\approx$30 keV) would be intermediate, as observed. It should be remembered that the measured intensity depends not only on $I(\phi)$ relative to a given direction, but also the number of electrons in the corresponding direction, and their energies, which we did not measure.

The fact that part of the emission came from the solid target is consistent with the argument. Although the electrons might suffer large angle deflections in the solid, the emission of high-energy Bremsstrahlung was mostly due to first deflections and thick target

Bremsstrahlung spectra were expected. Comparison of Figs. 5(b) and 6(a) suggests values of $\beta \approx 0.5$ or electrons of energy ~100 keV, consistent with the transmission data of the lead filters.

After compression, streak camera pictures show that the plasma blob proceeds upwards, away from the anode, with a velocity of several times 10^7 cm/s. The sheath was formed just after maximum compression because Fig. 4 shows that the plasma x rays appear slightly before the x rays from the anode. As the plasma moves upwards, it takes a few hundred nanoseconds before it expands sufficiently so that its density falls to a much lower value. During this period, the plasma could feed electrons near the axis into the sheath region, and if the electric fields were not dissipated, this may explain why x rays continued from the anode for hundreds of nanoseconds (Fig. 4). This picture is consistent with computer simulations of Hohl et al.,[19] and also with a suggestion for the mechanism of neutron production in a focus; namely, a converging beam model, proposed previously by one of the authors of Ref. 8. The same electric fields would accelerate the ions upwards and cause them to converge on the dense plasma blob. The majority of neutrons would be due to accelerated ions from the sheath colliding with those in the dense plasma target. The ions in the sheath should gain energies approaching 100 keV, the energy of the x rays, as they would have few collisions in the sheath. The emission of neutrons, however, depends on the plasma density in the focus and would only occur while the plasma remains compressed. Hence, neutron emission should discontinue after the plasma expands, but electrons might still be feeding into the sheath to give x-ray emission from the anode.

CONCLUSIONS

Measurements of the intensity of x-ray emission from a plasma focus show that low-energy (≈20 keV) x rays come from the plasma-focus region, but that the higher energy components (≈100 keV) come from the anode. The emission is anisotropic, the low-energy polar diagram resembling a cardioid, while the high-energy emission is a lobe into the anode, with a forward-to-back ratio of about 50. Consideration of the plasma parameters shows that even in the dense focus, the plasma should be near collisionless near the axis, with collisions even less likely in the region between the focus and the anode surface. Here, a sheath with strong electric fields could exist, and the electrons would be accelerated. By considering the radiation patterns of relativistic electrons a qualitative picture is obtained, which explains the measured polar diagrams, assuming the electrons that produce the x rays have velocity vectors lying roughly in a cone between the point of focus and the anode. Both the shape of the radiation patterns and the transmission data through filters imply electron energies of up to 100 keV. The average electron energy is, however, lower and probably about 3 keV at the focus, and about 10 keV on the anode surface. The picture is consistent with the converging beam model of neutron production, proposed previously.

ACKNOWLEDGEMENTS

The authors would like to thank Dr. Frank Hohl for valuable discussions and for his interest and support. The work was carried out at the National Aeronautics and Space Administration Langley Research Center, and supported in part under grants NAS1-11707-83, NAS1-1022, and NGR 43-002-034.

BIBLIOGRAPHY

1. D. P. Petrov, N. V. Filippov, T. I. Filippova, and V. A. Khrabrob, in "Plasma Physics and the Problems of Controlled Thermonuclear Reactions," (Pergamon, London, 1960), vol. IV, p. 198.
2. N. V. Filoppov, T. I. Filippova, and V. P. Vinogradou, Nucl. Fusion Suppl. 2, 566 (1962).
3. J. W. Mather, Bull. Am. Phys. Soc. 9, 177 (1963); 9, 339 (1964).
4. J. W. Mather, Phys. Fluids Suppl. 7, S28 (1964).
5. E. H. Beckner, J. A. P. 37, 4944 (1967).
6. E. H. Beckner, E. J. Clothiaux, and D. R. Smith, Phys. Fluids 12, 253 (1969).
7. H. L. L. van Paassen, R. H. Vandre and R. S. White, Phys. Fluids 13, 2606 (1970).
8. J. H. Lee, L. P. Shome, M. D. Williams, and H. Hermansdorfer, Phys. Fluids 14, 2217 (1971).
9. N. W. Jalufka and J. H. Lee, Phys. Fluids 15, 1954 (1972).
10. N. J. Peacock, P. D. Wilcock, R. J. Speer and P. D. Morgan, Third Conference on Plasma Physics and Controlled Nuclear Fusion Research, Novosibirsk, U.S.S.R., 1-7 August 1968.
11. M. J. Bernstein, D. A. Meskan and H. L. L. van Paassen, Air Force Report No. SAMSO-TR-69-304 of September 1969. Bernstein, M. J. Phys. Fluids 13, 2853 (1970).
12. J. H. Lee, D. S. Leobbaka, and C. E. Roos, Plasma Physics 13, 347 (1971).
13. H. A. Kramers, Phil. Mag 46 836 (1923).
14. R. C. Elton and A. D. Anderson, Naval Research Laboratory Report 6541 March 31, 1967.
15. J. R. Cameron, N. Suntharalingam and G. N. Keeney, "Thermoluminescent Dosimetry" (Wisconsin Press) 1968.

16. The equipment used was manufactured by the Harshaw Chemical co., 1945 E. 97 Street, Cleveland, Oh 44106.

17. H. Drieeer, Phys. Rev. 115, 238 (1959).

18. See for example, R. B. Leighton, "Principles of Modern Physics" McGraw Hill 1959, p. 413.

19. F. Hohl and S. Peter Gary, National Aeronautics and Space Administration Technical Note TN D7707, November 1974.

FIGURE CAPTIONS

Fig. 1. Experimental arrangement on the plasma focus device.

Fig. 2. (a) I(E) T(E) vs E. Continuous lines, T_c = 10 keV; dotted lines, T_c = 5 keV. The filters correspond to 2 mm of Al plus the following lead thicknesses in μm (1) 0, (2) 102, (3) 229, (4) 508, (5) 762.

(b) T_c vs R. R is the ratio of the signals through filters of 2 mm Al and 2 mm Al + 256 μm Pb, -curve A, 2 mm Al + 254 μm Pb and 2 mm Al + 762 μm Pb, -curve B. The curves A', B' correspond to an extra 100 μm Cu between the source and filters.

Fig. 3. Pinhole pictures of x rays taken through 2 mm Al (lower), 2 mm Al + 102 μm Pb (middle), and 2 mm Al + 254 μm Pb (upper).

(a) Single discharge $\theta = 80^{o}$

(b) 25 discharges superimposed $\theta = 0^{o}$

(c) 25 discharges superimposed $\theta = 80^{o}$

(d) TLD rasters corresponding to upper and lower pictures in (c).

Fig. 4. Time and space resolved x-ray measurements

(a) Oscilloscope trace showing x rays and neutron emission

(b) The light pipes were aligned on the middle image

(c) X ray signals from P and e respectively

Fig. 5. Polar diagrams for (a) medium energy x rays: ⊙ through aluminum (≃ 20 keV) ▲ through copper (≃ 30 keV)

(b) High energy x rays through Al (≃ 100 keV)

Fig. 6. (a) Radiation pattern for a single electron

(b) Electron trajectories

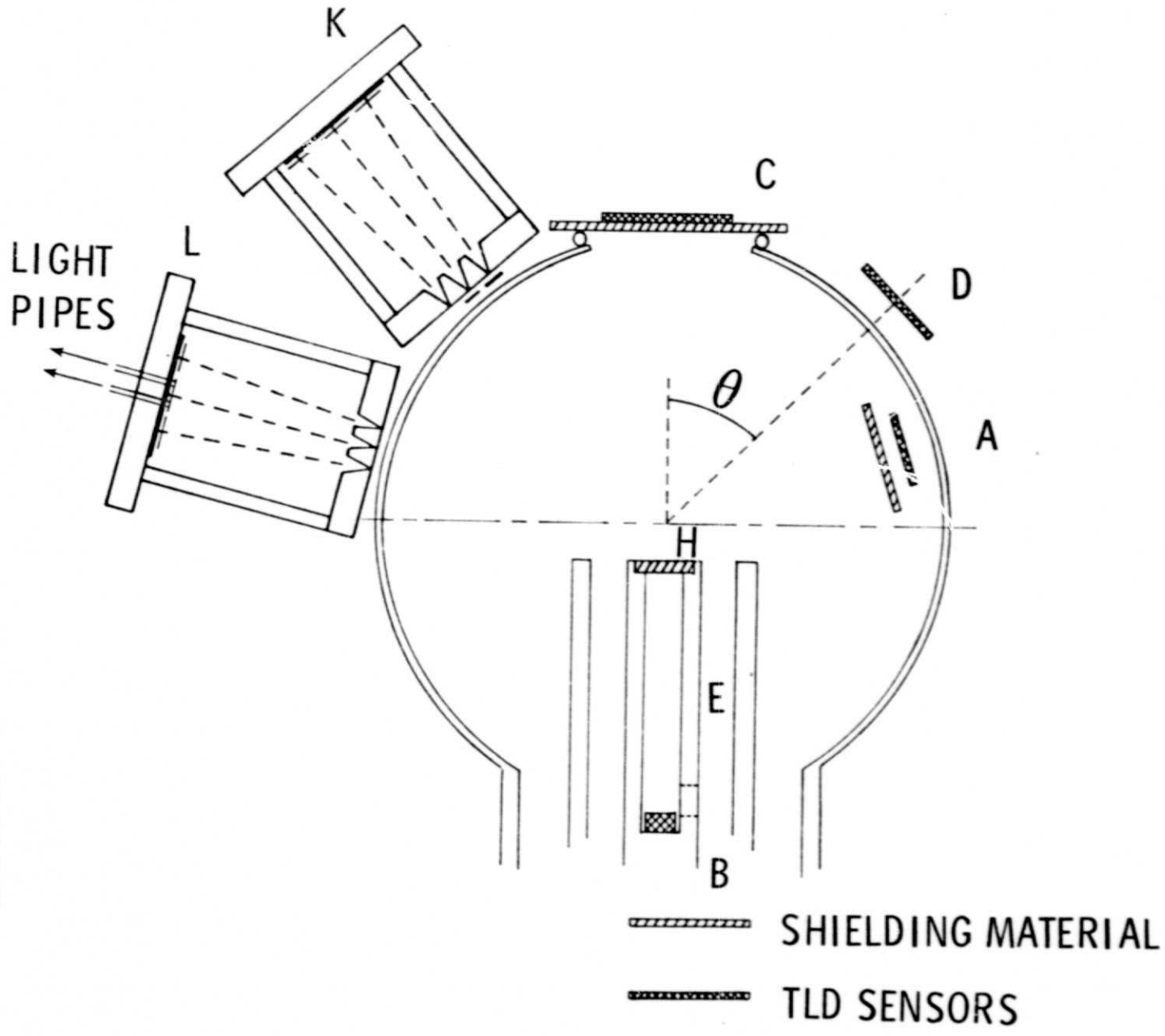

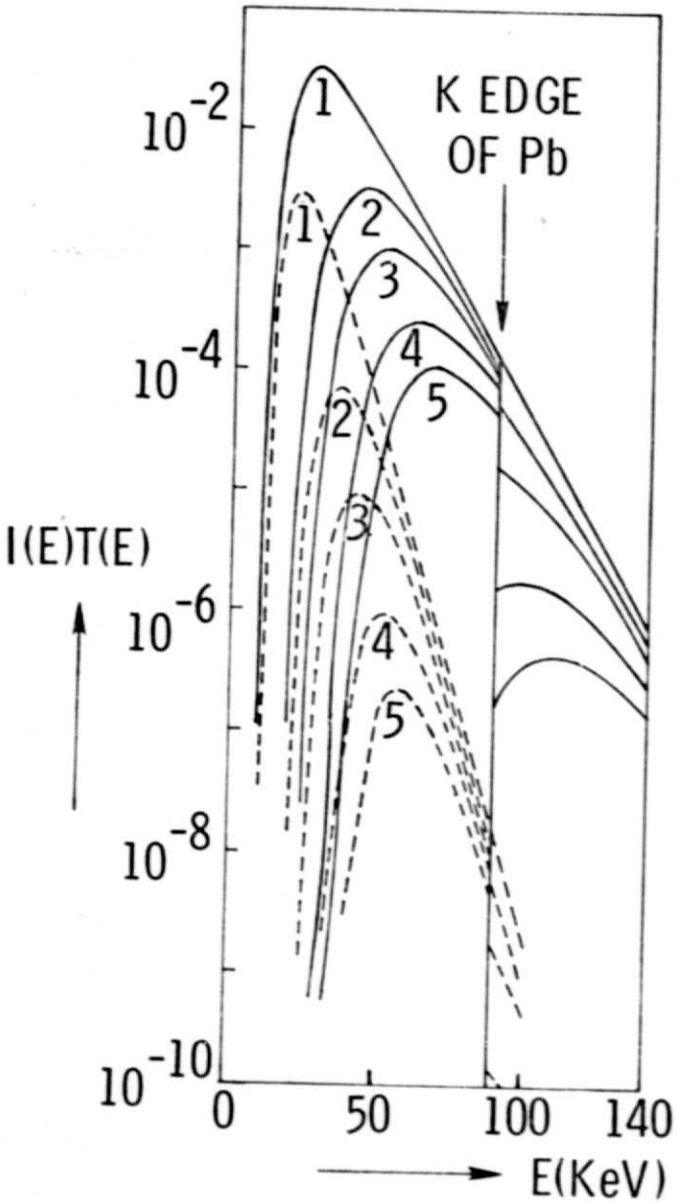
K EDGE
OF Pb
10^{-2}
10^{-4}
10^{-6}
10^{-8}
10^{-10}
I(E)T(E)
1
2
3
4
5
0
50
100
140
E(KeV)

(a)

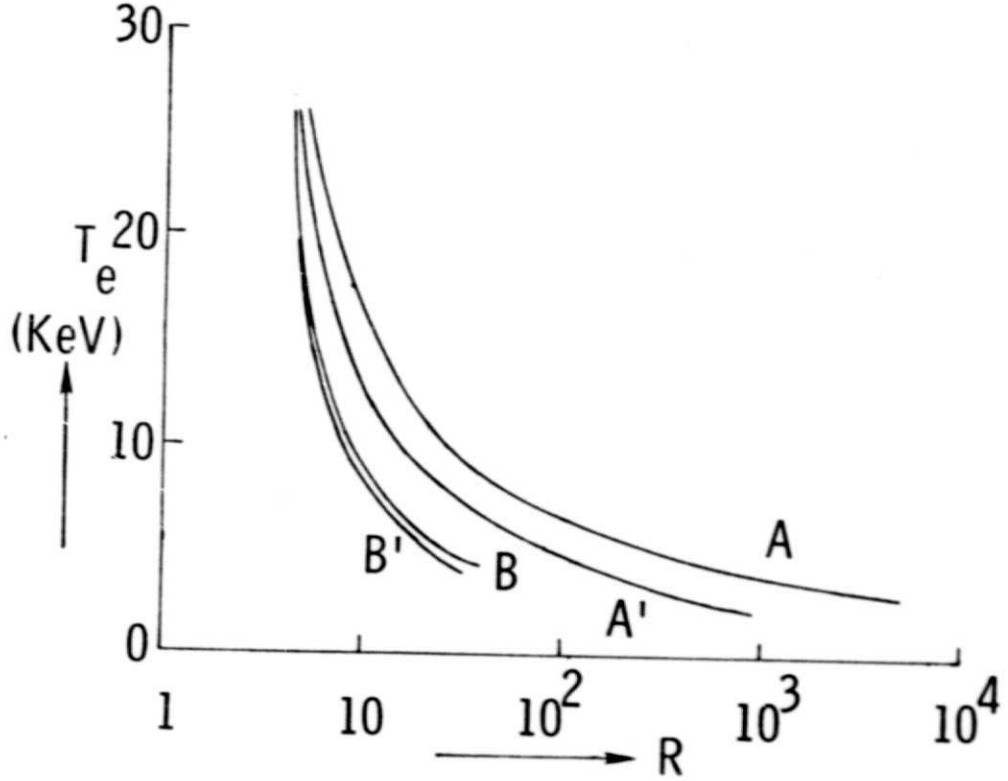
30
20
10
0
T_e
(KeV)
A
B'
B
A'
1
10
10^2
10^3
10^4
R

(b)

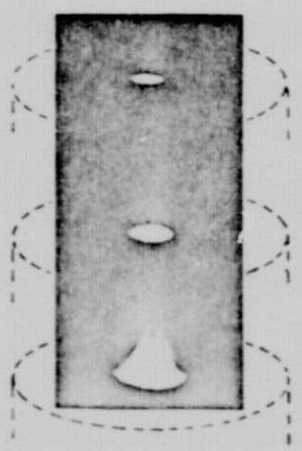

(a)

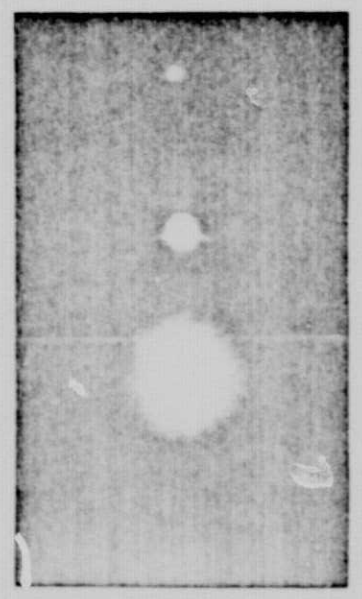

(b)

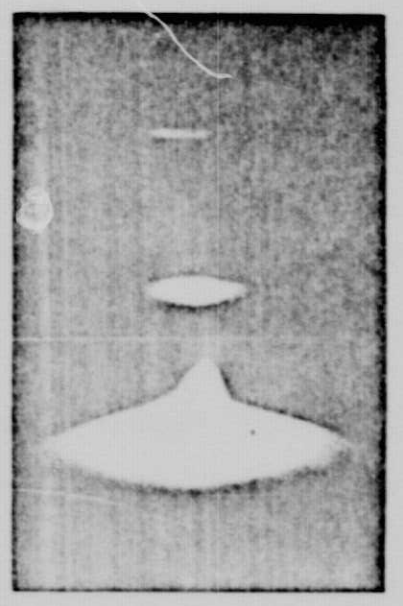

(c)

			41					
			45					
		18	118					
			9					

			5					
			366	167				
	[illegible]93	306	1130	1210	249	34		
359	815	1800	4050	4110	2000	903	351	96
114	231	460	1070	1220	574	346	200	111
			2	8	4	2		

(d)

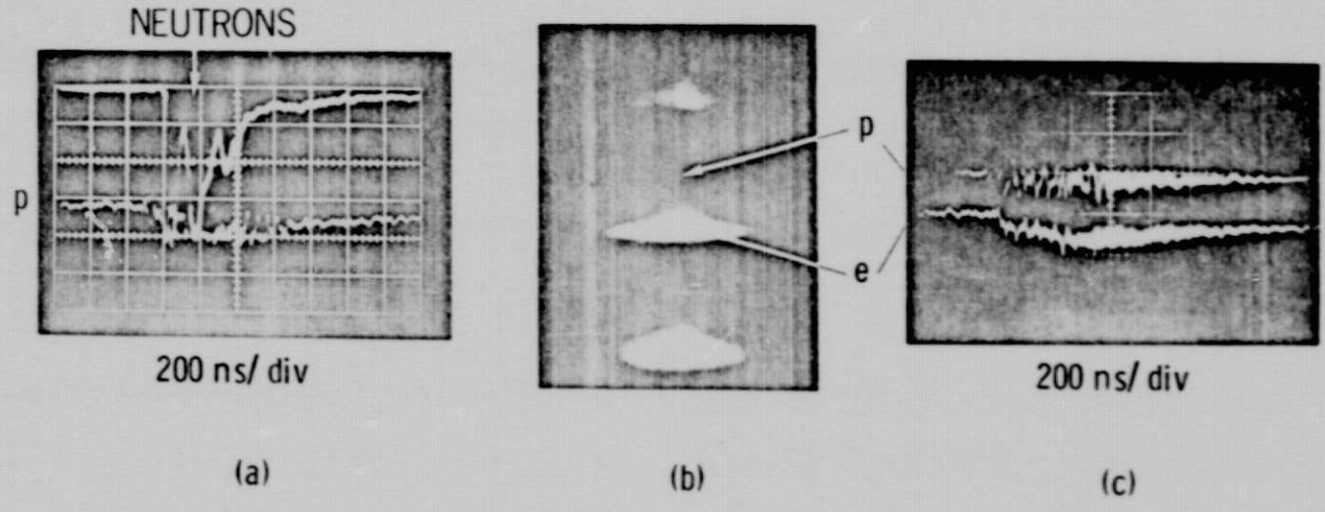
NEUTRONS
p
200 ns/ div
p
e
200 ns/ div
(a)
(b)
(c)

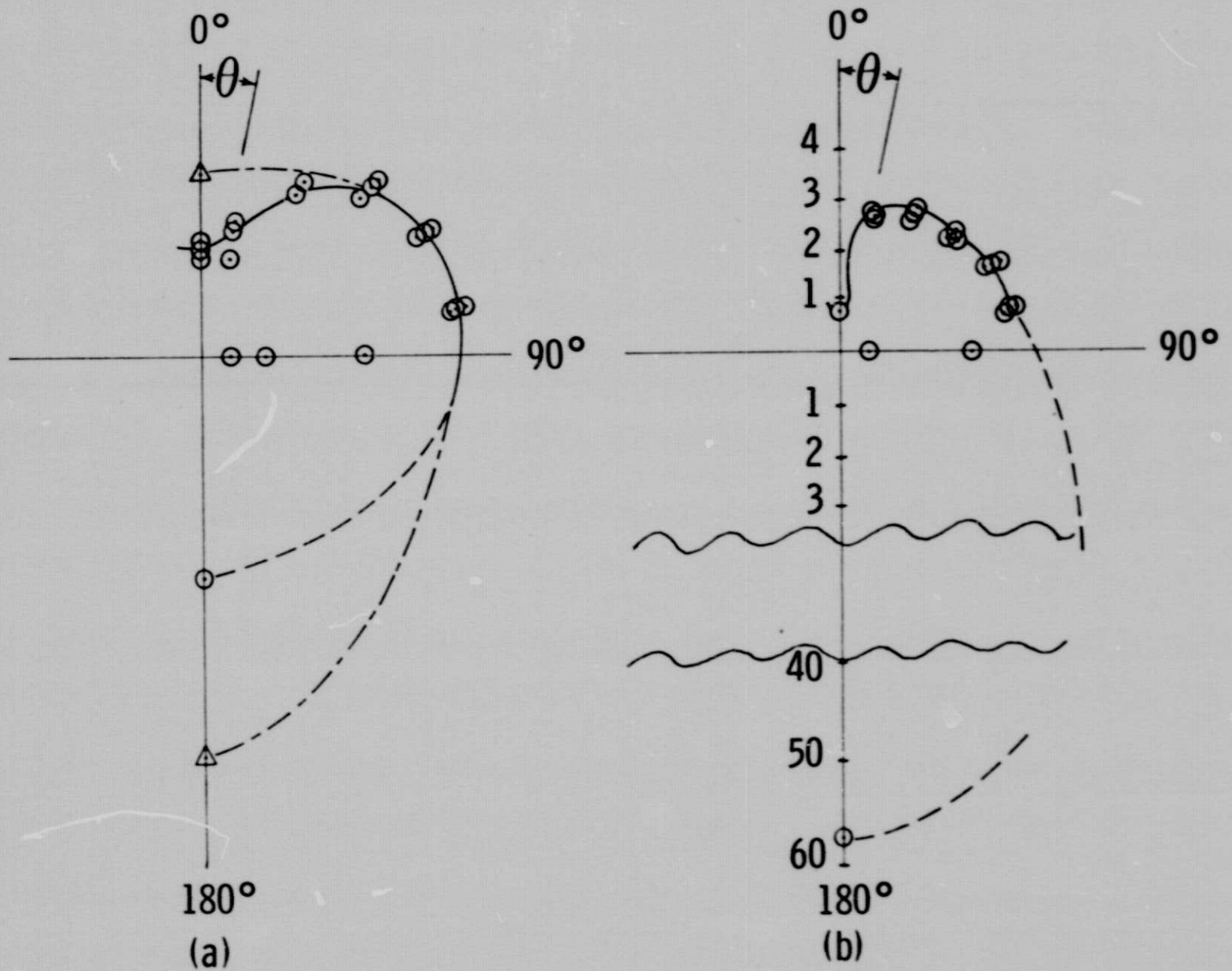
0°
θ
90°
180°
(a)
0°
θ
4
3
2
1
1
2
3
40
50
60
90°
180°
(b)

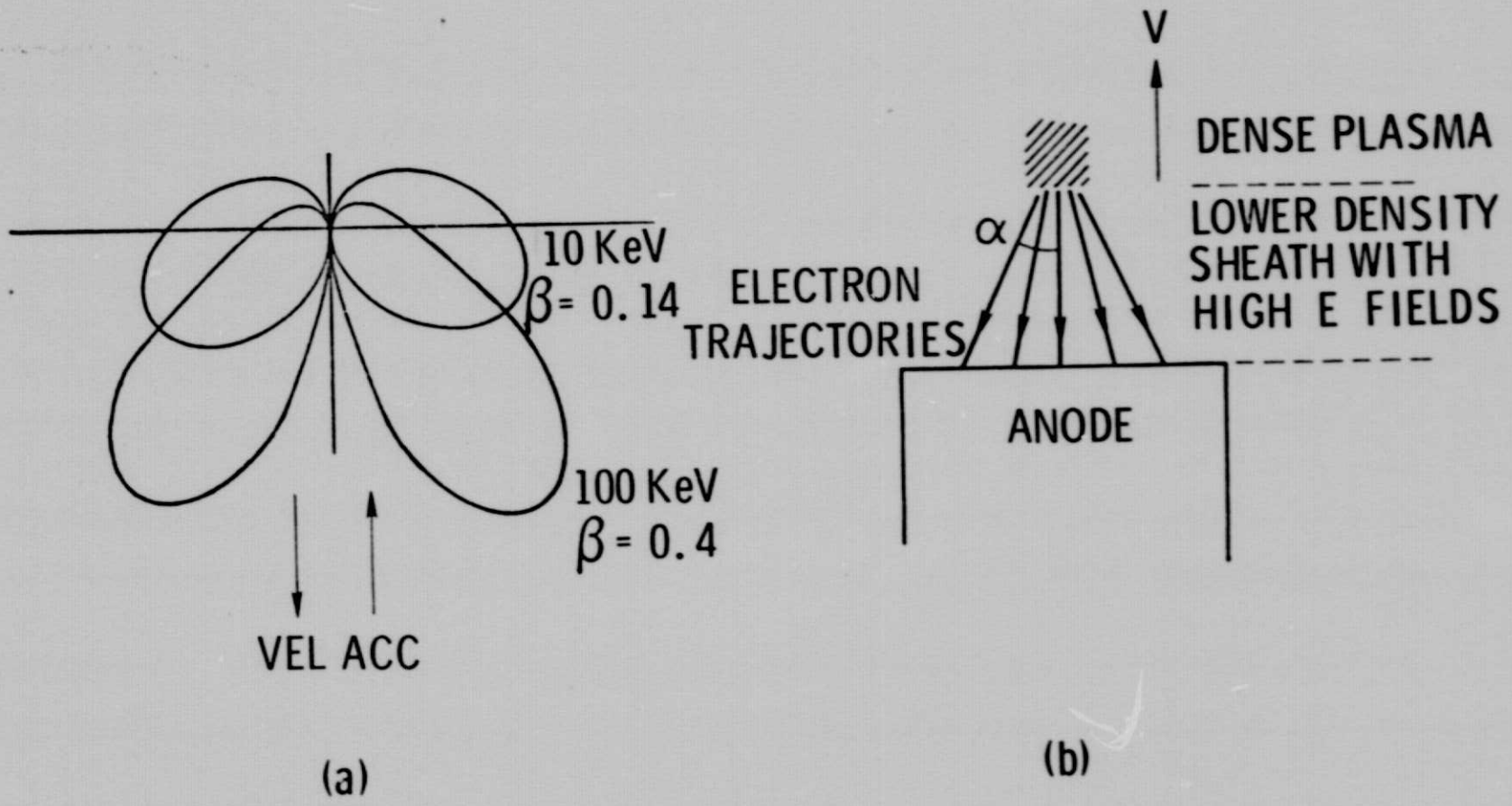
10 KeV
β = 0.14
100 KeV
β = 0.4
VEL ACC
(a)
V
DENSE PLASMA
LOWER DENSITY
SHEATH WITH
HIGH E FIELDS
α
ELECTRON
TRAJECTORIES
ANODE
(b)

APPENDIX B

HIGH ENERGY ELECTRON TRAJECTORIES IN A PLASMA FOCUS

One consequence of the proposed model in Appendix A is that the electrons producing the high energy x rays should have trajectories which are essentially straight lines lying in a cone (Appendix A, Figure 6). Therefore an experiment was performed to show whether the fast electrons in a focus traveled downwards, and if possible to check whether they traveled as a collimated beam or had angular spread.

The method consisted of detecting the electrons by the x rays they emitted (Figure 1). A hollow anode with a hole of about 4-mm diameter was constructed of aluminum, a material relatively transparent to x rays. Triple pinhole cameras were placed at C and D some 15 cm from the focus, to record the x rays. The diameter of the pinholes was 0.4 mm minimum to give adequate resolution, and a DuPont Chronex, Lightning type x-ray detector screen was placed about 15 cm behind them. The screen emitted visible radiation when struck by the x rays and Polaroid ASA 10 000 speed film was placed behind it to give contact prints.

If the fast electrons traveled downwards, then x-ray emission would delineate the hole on the upper surface at A and if they continued downwards the outline of the hole should appear at B, as x rays from the bottom of the cavity. Both cameras observed region A through the 2-mm aluminum vacuum vessel and observed B through the upper surface of the anode as well — an additional 2 mm (or less because of erosion) of aluminum. In Figure 2(a) the radiation from six focuses was superimposed, and the lower picture, with no lead filter, shows low energy x rays of around 20 KeV emitted from a large area of the upper anode surface. The middle picture recorded through 250 μm, and the upper picture through 500 μm of lead, thus recording x rays of

greater than about 30 and 50 KeV, respectively. The higher energy x rays are emitted from the center of the anode. These pictures are in agreement with Appendix A, Figure 3(c) and show that the presence of the hole in the anode, and material of aluminum rather than copper, did not alter the characteristics of the focus. Emission from region B is not apparent however.

Filters of 250 μm of lead were then placed over all the pinholes, to record x rays of about 30 KeV and over. The results of superimposing the x rays from eight focuses on camera C at an angle of about 50° to the vertical axis are shown in Figure 2(b). In the three pictures, identical except for a small difference in angle of viewing, the hole is evident from the ring of x rays from surface A, and its image at B can be seen at the correct position below it. Similar results were obtained for camera D. The size of the hole has been enlarged by the subsequent discharges.

The geometry suggests that a more or less collimated beam of fast electrons entered the cavity, and that the angular spread is small. On the other hand, some other data pictures showed slight radiation from the outer edges of the flat surface B, suggesting that whereas the bulk of the electrons were collimated, nevertheless there were a few in the cavity traveling at large angles to the axis. Essentially however, the model proposed in Appendix A seems confirmed.

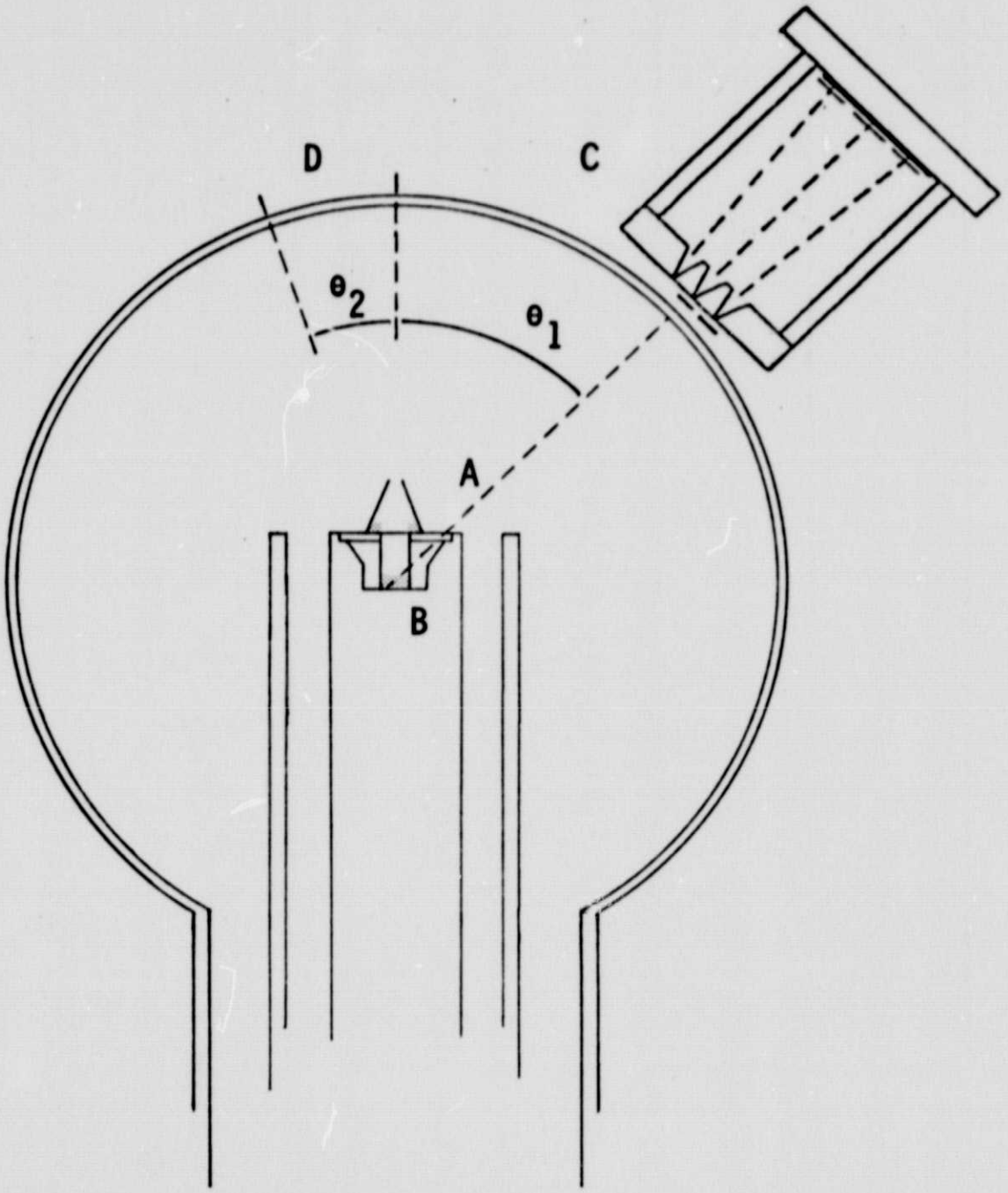

Fig. 1. - Experimental arrangement.

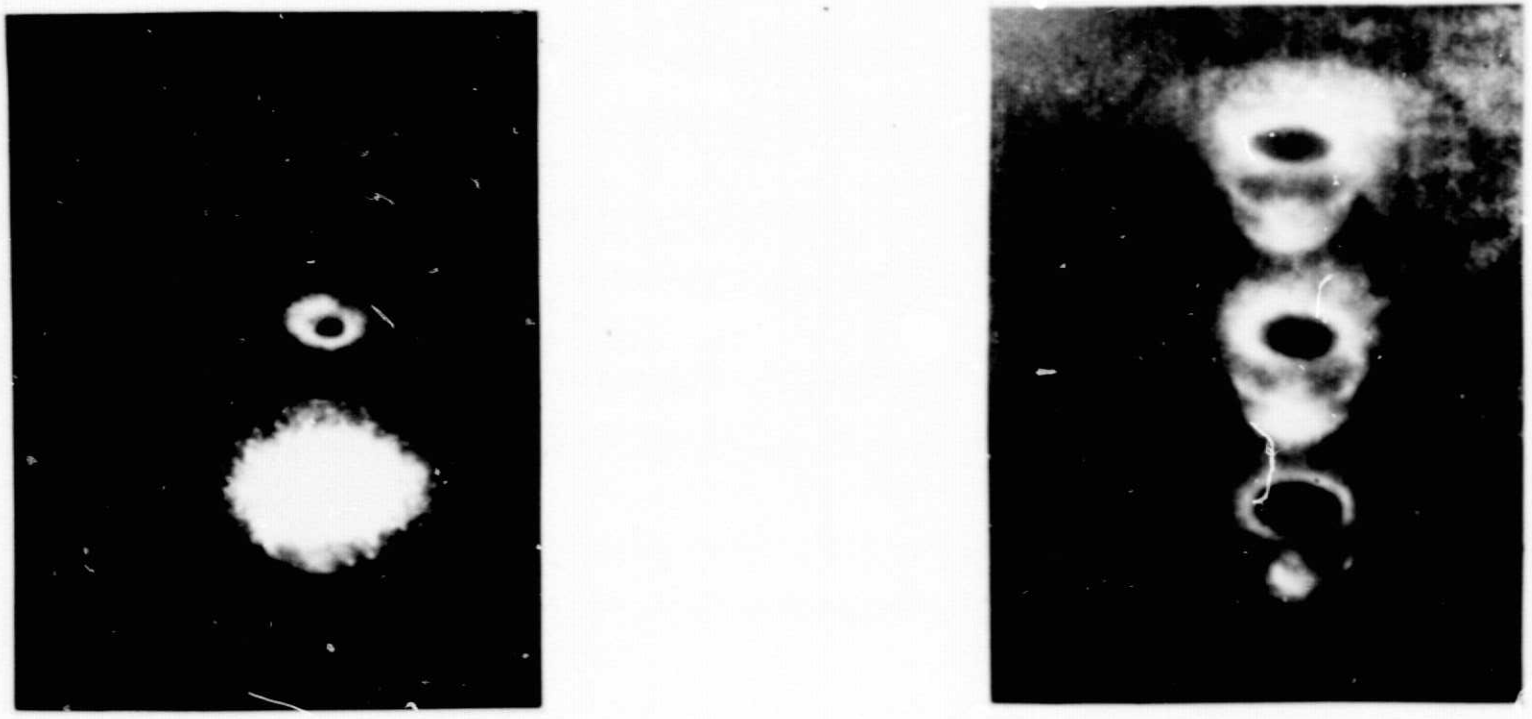

(a) (b)

Fig. 2. - Triple pinhole pictures from camera C.
(a) The lower picture is taken through the vacuum vessel;
the middle and upper through 250 and 500 µm of lead in addition.
(b) All three pinholes are covered with 250 µm lead.

APPENDIX C

MEASUREMENT OF NEUTRON EMISSION FROM A PLASMA FOCUS

1. Introduction

The mechanism of x-ray emission proposed in Appendix A suggests that electric fields exist in the sheath region between the dense plasma and the anode. Such fields should accelerate ions to energies of order 100 KeV and these relatively few ions might be responsible for the main neutron production. This picture is in accord with the converging beam model for neutrons, proposed already.

The purpose of this experiment was to determine where the neutrons originated in space, and hence possibly infer the fast ion trajectories.

2. Experimental Method

Unfortunately, pinhole techniques cannot be applied to neutrons, so therefore a boron filled polyethylene collimator was used. This was placed outside the vacuum vessel (Figure 1) and was 6" long and 6" diameter and had holes of 40 mils diameter spaced 1/8" apart, in a two-dimensional array. An interposed lead shield, some 250 μm thick, helped reduce the effect of x rays. The neutrons were recorded on a sensor at B and two kinds of sensors were tried.

The first type consisted of plastic scintillators of NE 102 in the form of thin rods, 3" long and 40 mils diameter, placed inside the collimator holes at CD. The scintillators should produce visible light when struck by neutrons, and the ends D were photographed. The light intensity was too low for a camera using 10 000 ASA film with an f 1.9 lens focused on B, and therefore a contact print was tried at B, using available 3000 ASA film. A run of 50 focuses did produce a very faint image, but with not too conclusive results.

The second type of sensor used was a raster of type 600 thermoluminescent detectors (TLD). These were crystals of 1/8 × 1/8 × 1/32 inches, and a 24 × 4 array covered an area 3 inches by 1/2 inch adequate for surveying the focus. Their size coincided with the spacing of the collimator holes. Rasters of type 400 TLD's had been used already to record x-ray emission (Appendix A, Figure 3) and type 600 should record neutrons.

A. Separating the x rays from the neutrons. In principle, lead filters should reduce the x rays and allow neutrons through, but we found that lead also reduced the neutron signal. Thus, the question arose what would be the optimum thickness of lead to record neutrons accurately, and second, what fraction of the signal on the TLD 600's was due to x rays rather than neutrons.

TLD's were subjected to the emission of 31 focuses, and the responses recorded as a function of thickness of filters of both lead (0, 100, 200, 300, 500 and 750 μm) and boron-filled polyethylene (0, 5, 10, 15 cm) and combinations of these materials. Both type 400 which should measure mainly x rays, and the type 600, which should measure mainly neutrons were used. Figure 2(a) shows the response vs. thickness of lead, with and without 5 cm of polyethylene. Each point was recorded on three TLD's and the readings show good consistency. The polyethylene reduces the signal by a factor of about two for all the readings on the TLD 400's, which would be consistent with them recording mainly x rays. The figure shows that for the type 600, 300 μm of lead reduced the signal by about 100. Above this thickness, the polyethylene reduced the signal by a further factor of 10 or more, suggesting that the contribution here was mostly neutrons. Hence lead of about 300 μm was used with the TLD 600's and we believe they recorded neutrons rather than x rays, with probably about 90° of the signal due to neutrons.

B. Experimental Results. With these conditions, two runs were made but the recorded signals were small and hardly above the noise level, even when as many as 60 focuses were superimposed. Both results suggested the neutrons are produced near the dense focus or on the side away from the anode. The experiment is being repeated with a greater number of focuses superimposed.

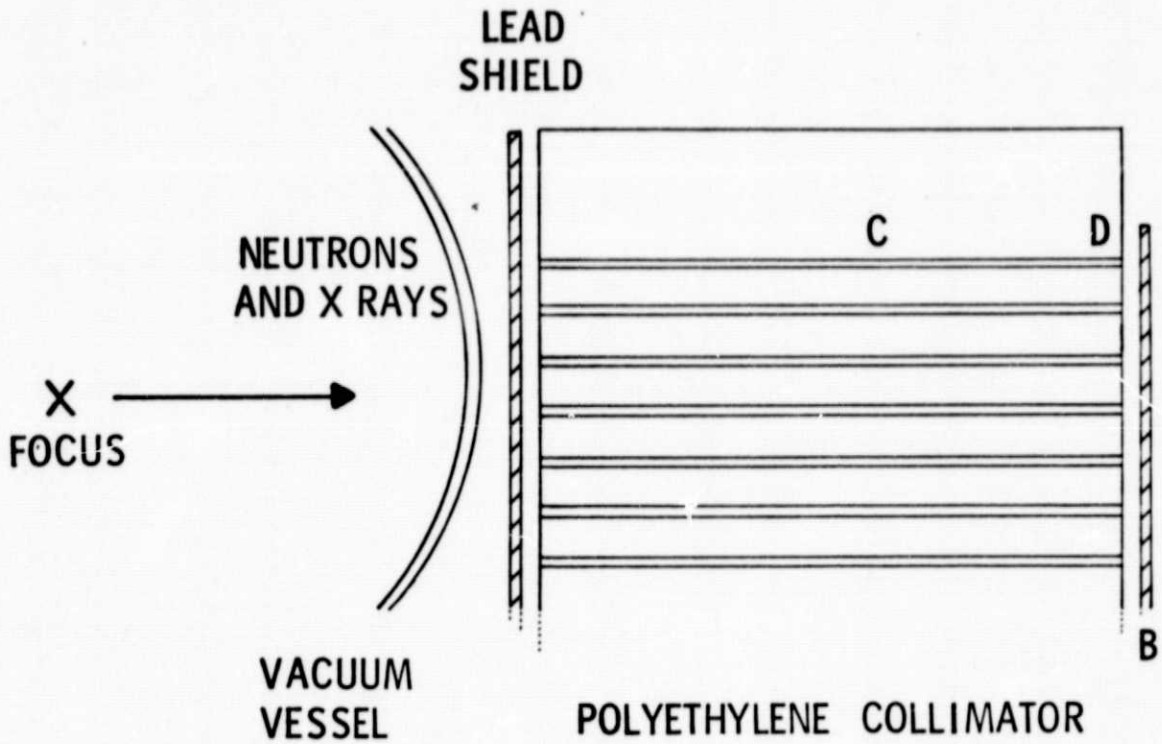

Fig. 1. - Method of detecting neutrons.

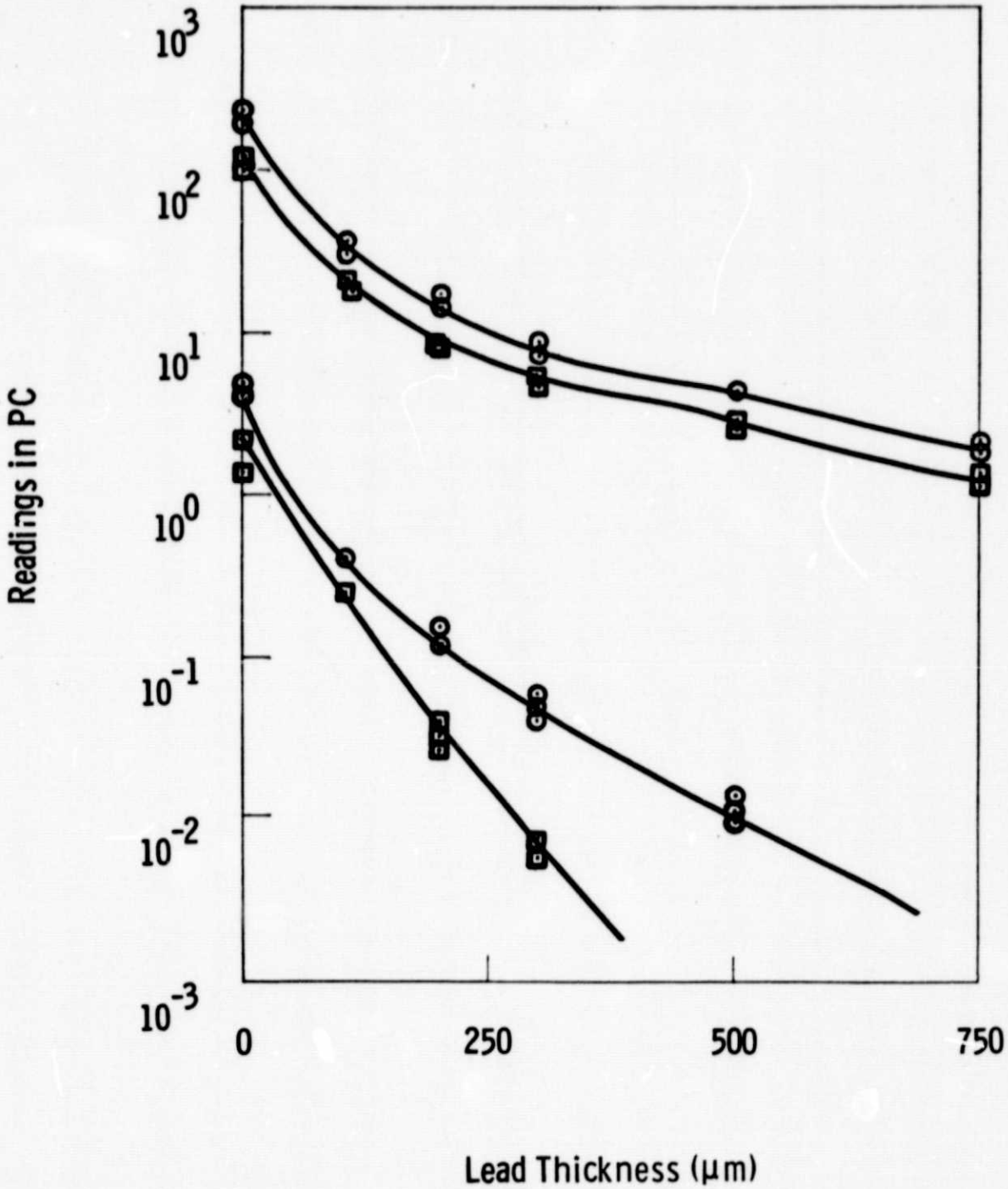

Fig. 2. - Response of TLD 400, and TLD 600, to x rays and neutrons from 31 focuses vs thickness of lead filters, ⊙ without, ⊡ with additional 2" of boron-filled polyethylene.

APPENDIX D

POSSIBLE FUTURE EXPERIMENTS

1. Emission of X rays vs. Space and Time

To obtain space (one dimensional) and fast time response of x-ray emission, a lead collimator with a line of holes which can hold NE 102 scintillator rods has been constructed. Preliminary attempts were made to record the light output on an STL streak camera. The light output was too low for an STL 500 camera using its normal lenses. Possibilities are to use the faster type Imacon camera, which is 100 times more sensitive, or as a last resort, place the scintillators against its photo cathode.

2. Measurements of Neutrons and Hard X-rays vs. Space and Time using Time-of-Flight Separation

A time-of-flight detector has been used successfully on Focus I for some time. The sensor is a 6" slab of NE 102 covered with 1/8" lead, and the light output is detected by a photomultiplier vs. time. Hard x rays and neutrons are both recorded but the path of 3 m causes a time difference of 150 ns -- adequate to separate the signals. The ease of using photomultipliers with their high sensitivity suggests a combination of the time-of-flight technique and collimators to provide spatial discrimination in addition.

An arrangement for measuring neutrons vs. time and space is shown in Figure 1. The polyethylene collimator, 15 cm long, is clamped adjacent to the vacuum vessel and one hole is chosen which accepts radiation from a small region of the focus. A lead shield C and a 15-cm slab of polyethylene D eliminates radiation from the other holes. (The use of the array of holes in the collimator may be preferable to using a moveable single hole as relative positioning is exact.)

The first question is the reduction of signal because of collimation. The photo cathode of the photomultiplier is 4.4-cm diameter and at a distance

of 3 m, while the collimator hole is 100 μm diameter, and distance AC is 30 cm. The ratio of the solid angle subtended by the hole to that subtended by the photocathode is 5×10^{-2} and as 10 V signals are common at present, a single hole should give signals of order 0.5 v, well above noise level.

The second question is the resolution in space at the focus, which is satisfactory, as a circle of order 3-mm diameter is delineated. Thirdly, the radiation through the hole diverges, but at 3 m it spreads to a circle 4 cm in diameter, and can all be collected by the photo cathode. However, the photo cathode should be carefully aligned to be on axis for any particular hole.

To obtain spatial resolution, different holes would be exposed shot to shot, but because of shot to shot variations, a second similar detector should be used observing the whole plasma, and used for normalization. The method requires fewest changes from the present experimental set-up.

3. Time of Flight Ion Velocity Analyzers

If the fast ions travel away from the anode, they might be detected outside the vacuum vessel in a time-of-flight analyzer. Preliminary estimates suggest a path length of 3m -- feasible on Focus II. The device would consist of a long tube differentially pumped with a Rogowski coil sensing the entrance of the ions, and a Faraday cup collecting them at the other end. The signals vs. time would permit an estimate of the ion velocity distribution.

4. Measurements of Neutron Flux vs. Angle

The TLD's can define angle of collection to within about 1°. Previous measurements with photomultipliers can be easily confirmed, as well as measurements made behind the anode (similar to the x-ray measurements in Appendix A) using TLD 600's shielded with a lead filter, to detect neutron flux vs. angle.

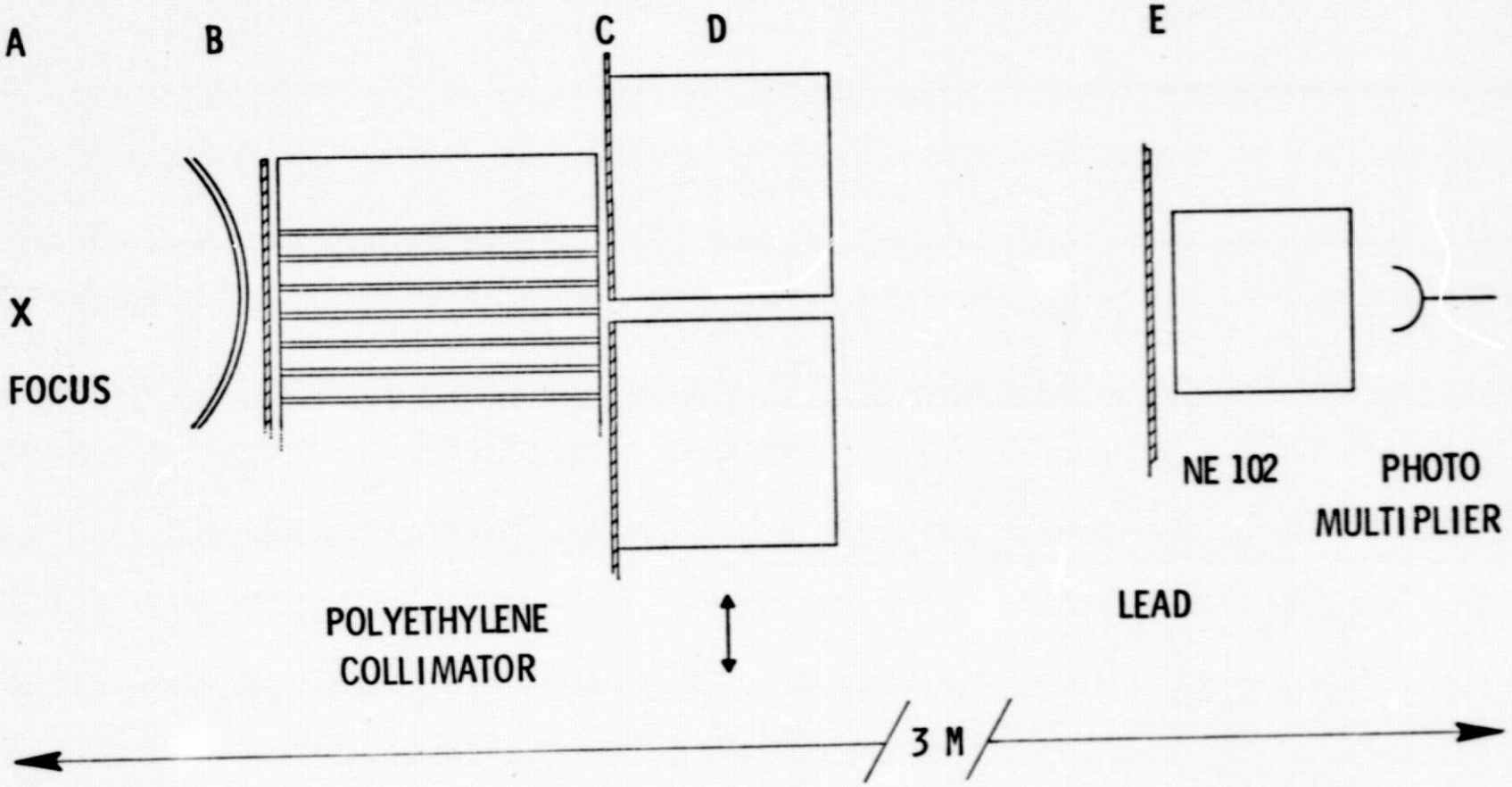

Fig. 1. - Method of measuring neutrons vs space and time using time-of-flight separation from x-ray signal.